Nuclear Overhauser Effect Studies on the Conformation of Magnesium Adenosine 5′-Triphosphate Bound to Rabbit Muscle Creatine Kinase†

Paul R. Rosevear,*,‡ Vincent M. Powers,§ David Dowhan,‡ Albert S. Mildvan,∥ and George L. Kenyon§

Department of Biochemistry and Molecular Biology, University of Texas Medical School at Houston, Houston, Texas 77025, Departments of Pharmaceutical Chemistry and of Biochemistry and Biophysics, University of California, San Francisco, California 94143, and Department of Biological Chemistry, The Johns Hopkins University School of Medicine, Baltimore, Maryland 21205

Received February 6, 1987; Revised Manuscript Received April 29, 1987

ABSTRACT: Nuclear Overhauser effects were used to determine interproton distances on MgATP bound to rabbit muscle creatine kinase. The internuclear distances were used in a distance geometry program that objectively determines both the conformation of the bound MgATP and its uniqueness. Two classes of structures were found that satisfied the measured interproton distances. Both classes had the same anti glycosidic torsional angle ($\chi = 78 \pm 10°$) but differed in their ribose ring puckers (O1′-endo or C4′-exo). The uniqueness of the glycosidic torsional angle is consistent with the preference of creatine kinase for adenine nucleotides. One of these conformations of MgATP bound to creatine kinase is indistinguishable from the conformation found for $Co(NH_3)_4ATP$ bound to the catalytic subunit of protein kinase, which also has a high specificity for adenine nucleotides [$\chi = 78 \pm 10°$, O1′-endo; Rosevear, P. R., Bramson, H. N., O'Brian, C., Kaiser, E. T., & Mildvan, A. S. (1983) *Biochemistry 22*, 3439]. Distance geometry calculations also suggest that upper limit distances, when low enough (≤3.4 Å), can be used instead of measured distances to define, within experimental error, the glycosidic torsional angle of bound nucleotides. However, this approach does not permit an evaluation of the ribose ring pucker.

Creatine kinase is a dimeric enzymic (M_r 86 000) that catalyzes the reversible phosphorylation of creatine by MgATP (Kenyon & Reed, 1983). This enzyme plays an important role in energy metabolism, and much information exists on the kinetic mechanism (Morrison & James, 1965; Morrison & Cleland, 1966; Schimerlik & Cleland, 1973; Hammes & Hurst, 1969), on the location of the divalent cation activator (Reed & Leyh, 1980; Leyh et al., 1985), and on the nature and role of certain amino acid residues at or near the active site (James & Cohn, 1974; Cook et al., 1981; Rosevear et al., 1981). Proton NMR studies of six of the 17 histidine residues per subunit of creatine kinase have suggested that one of the histidines, designated His-2,[1] functions as the general acid/base catalyst that deprotonates the guanidinium group of creatine as it is phosphorylated by MgATP (Rosevear et al., 1981). The pK values of His-2 and the effects of substrates on this pK are in quantitative agreement with the results of a pH–rate study on creatine kinase (Cook et al., 1981). Histidine residues had previously been implicated in catalysis by chemical modification with diethyl pyrocarbonate (Pradel & Kassab, 1968; Clarke & Price, 1979).

Chemical modification with butanedione has suggested the presence of an arginine residue at the active site (Borders & Riordan, 1975). Fluorescence quenching and NMR studies have suggested the presence of one or more aromatic residues, possibly a tryptophan (James, 1976; Vasak et al., 1979), as well as a lysine (James & Cohn, 1974) and a histidine residue (Rosevear et al., 1981) at the nucleotide binding site. However, the location of these residues in the amino acid sequence and their precise roles in substrate binding and catalysis remain to be established.

An important prerequisite to a complete understanding of the enzymatic mechanism is the elucidation of the arrangement and conformations of the substrates in the various enzyme–substrate complexes. Such information is needed to understand the specific structural constraints within the enzyme–substrate complex that are important both in catalysis and in specificity.

Distances from a nitroxide-spin-labeled sulfhydryl group have been used to position the nucleotide and creatine substrates with respect to the spin-label (McLaughlin et al., 1976). Reed and Leyh (1980) and Leyh et al. (1985) have also established tridentate coordination of the divalent cation activator by the three phosphoryl groups of ATP. However, little information is currently available on the conformation of ATP at the active site of creatine kinase.

NMR methods have been widely used to determine the conformations and arrangements of flexible substrates bound at the active sites of enzymes (Mildvan et al., 1980; Clore & Groneborn, 1983; Mildvan et al., 1983; Levy et al., 1983; Rosevear et al., 1983). Recently, the NOE[2] method has been used to determine the conformations of a number of enzyme-bound nucleotide substrates (Clore & Groneborn, 1983; Rosevear et al., 1983, 1987; Levy et al., 1983; Fry et al., 1985; Ferrin & Mildvan, 1985, 1986). In this paper, we have used the NOE method and computer modeling studies to determine the conformation of MgATP bound to creatine kinase. In-

† This work was supported by National Institutes of Health Grants AM-28616 to A.S.M. and AR-17323 to G.L.K. and Robert A. Welch Foundation Grant AU-1025 to P.R.R. V.M.P. is a Fellow of the American Foundation for Pharmaceutical Education.

* Author to whom correspondence should be addressed.
‡ University of Texas Medical School at Houston.
§ University of California.
∥ The Johns Hopkins University School of Medicine.

[1] This histidine residue has been designated as "His-2" since its C-2 proton is the second most downfield shifted in the protein's proton NMR spectrum at 250 MHz (Rosevear et al., 1981).

[2] Abbreviations: NOE, nuclear Overhauser effect; DSS, sodium 4,4-dimethyl-4-silapentane-1-sulfonate; SDS, sodium dodecyl sulfate; DTT, dithiothreitol.

0006-2960/87/0426-5338$01.50/0

ternuclear distances determined from the NOE studies were used in a modified distance geometry algorithm to calculate the conformation of enzyme-bound ATP from known and measured interatomic distances (Kuntz et al., 1979; Havel et al., 1983; Rosevear et al., 1984). Two classes of ATP structures at the active site were found that satisfied the interproton distances, but that differed in their ribose sugar puckers. Both classes had identical glycosidic torsional angles ($\chi = 78 \pm 10°$). The conformation of enzyme-bound MgATP thus determined is consistent with the previous distances determined from a paramagnetic nitroxide spin-label to protons of bound MgADP (McLaughlin et al., 1976).

Experimental Procedures

Materials. Tris-d_{11} [tris(hydroxymethyl)aminomethane-d_{11}] was obtained from MSD Isotopes. ATP, ADP, creatine, phosphocreatine, and NADH were purchased from Sigma. Pyruvate kinase and lactate dehydrogenase were obtained from Boehringer Mannheim.

Methods. Creatine kinase was purified by the method of Hershenson et al. (1986) and stored in 50 mM Tris–acetate buffer, pH 8.0, containing 10 mM DTT. The enzyme had an activity of 103 units/mg when assayed by the coupled pyruvate kinase and lactate dehydrogenase assay (Tanzer & Gilvarg, 1959) and was >95% pure by SDS–polyacrylamide gel electrophoresis. The concentration of creatine kinase was determined spectrophotometrically with $A_{280} = 8.8$ (Noda et al., 1954) and a M_r of 86 000. The enzyme was concentrated and deuteriated in an Amicon cell with a PM10 membrane by repeated concentration and dilution in 10 mM Tris-d_{11}, pH 8.0, containing 0.1 mM DTT at 4 °C. The typical NMR experiment contained 1.3 mM rabbit muscle creatine kinase sites, 14.5 mM ATP, and 27 mM $MgCl_2$ in a total volume of 0.43 mL.

Magnetic Resonance Methods. ^{1}H NMR spectra were obtained on a GN 500 NMR spectrometer with 16-bit A/D conversion. Chemical shifts were relative to external DSS. The time dependence of the nuclear Overhauser effect was measured with the pulse sequence

$$(\text{RD–preirradiate}[t,\omega]\text{–observation pulse})_{16n}$$

where RD is the relaxation delay, t is the duration of preirradiation, ω is the frequency of the irradiated resonance, and n is the number of frequencies irradiated. To ensure complete relaxation between observation pulses, a relaxation delay of $>7T_1$ was routinely used. The proton decoupler was utilized to produce a selective preirradiation pulse of desired duration, t, usually between 50 and 500 ms. The NOE was observed by subtraction of the control FID from the experimental FID, and the differnce FID was Fourier transformed and phased to give positive peaks for negative NOEs. The magnitude of the NOE was determined either by peak height measurement or by peak integration, which gave indistinguishable results (Rosevear et al., 1983, 1987).

The ribose H2′ resonance of ATP was obscured by the HDO signal and could not be directly observed in the presence of creatine kinase. The chemical shift of the ribose H2′ resonance was therefore determined by searching for a frequency that, upon preirradiation, gave a negative NOE to the ribose H1′ resonance. Model building and X-ray studies indicate that the ribose H1′ to H2′ distance lies within the limits of 2.9 ± 0.2 Å, regardless of either the ribose conformation or the glycosyl torsional angle (DeLeeuw et al., 1980; Levitt & Warshell, 1978; Rosevear et al., 1983). Thus, regardless of the conformations of ATP bound to creatine kinase, a negative NOE is always expected between these two protons.

Longitudinal relaxation rates ($1/T_1$) were measured by selective saturation of individual resonances and monitoring of their recoveries (Tropp & Redfield, 1981). Transverse relaxation rates ($1/T_2$) were calculated from the line width at half-height ($\Delta\nu$) according to the relation $1/T_2 = \Pi\Delta\nu$.

Internuclear NOEs on bound MgATP were measured by selectively preirradiating the H1′, H2′, H3′, H4′, H5′, H5″, and H8 protons for varying times and observing the time-dependent changes in the magnitization of the monitored MgATP resonances. This approach allows discrimination between primary and secondary effects, since the latter display a longer lag period before development of the NOE. The magnitude of the final steady-state NOE from spin B to spin A will depend on the competition between σ_{AB} (s^{-1}), the cross-relaxation rate or the rate that energy is transferred from spin B to spin A, and ρ_A (s^{-1}), the spin–lattice relaxation rate of spin A. As previously shown (Wagner & Wuthrich, 1979; Rosevear et al., 1983) for a two-spin system, the cross-relaxation rate (σ_{AB}) can be calculated from the time dependence of the NOE and the selective longitudinal relaxation rate of spin A (ρ_A) (eq 1). In eq 1, $f_A(B)$ is the NOE to spin A upon

$$f_A(B)_t = \frac{\sigma_{AB}}{\rho_A}(1 - e^{-\rho_A t}) + \frac{\sigma_{AB}}{\rho_A - c}(e^{-\rho_A t} - e^{-ct}) \quad (1)$$

preirradiation of spin B for time t (s), and c (s^{-1}) is the rate constant for saturation of spin B, which is approximated by $(1/2)(1/T_{1B} + 1/T_{2B})$ (Wagner & Wuthrich, 1979).

The time dependencies of the NOEs from each of the selectively preirradiated protons to the observed protons were fit with eq 1 by nonlinear regression analysis using the experimentally determined $f_A(B)$ and ρ_A values and varying both σ_{AB} and c. Values of c were found to vary between 16 and 30 s^{-1} and did not significantly alter the values of σ_{AB}. The calculated cross-relaxation rate (σ_{AB}) and the correlation function [$f(\tau_r)$] are used to calculate the distance between nucleus A and nucleus B (r_{AB}) in angstroms with eq 2. In

$$r_{AB} = D\left[\frac{f(\tau_r)}{\sigma_{AB}}\right]^{1/6} \quad (2)$$

eq 2 the constant D, $(\gamma^2h^2/10)^{1/6}$, is numerically equal to 62.02 Å $s^{-1/3}$ if A and B are protons and the correlation function $f(\tau_r)$ is given by eq 3, where ω_I is the nuclear precession fre-

$$f(\tau_r) = \frac{6\tau_r}{1 + 4\omega_I^2\tau_r^2} - \tau_r \quad (3)$$

quency and τ_r (s) is the correlation time. Equations 2 and 3 assume isotropic rotation of the molecule as a whole with a time constant τ_r shorter than any time constants of internal motion (Kalk & Berendsen, 1976). This approximation was justified by the results. The correlation time was calculated by assuming a fixed distance, independent of conformation, of 2.9 ± 0.2 Å between ribose H1′ and H2′ (Rosevear et al., 1983). Use of a single correlation time to calculate all internuclear distances makes the assumption that all internuclear vectors in ATP have the same correlation time as that found between ribose H1′ and H2′. The correlation time can also be estimated with eq 4 from the ratios (T_1/T_2) of the longi-

$$\frac{T_1}{T_2} = \frac{12\omega_I^4\tau_r^4 + 37\omega_I^2\tau_r^2 + 10}{16\omega_I^2\tau_r^2 + 10} \quad (4)$$

tudinal and transverse relaxation rates (Solomon, 1955).

Distance Geometry Method. The distance geometry approach (Kuntz et al., 1979; Rosevear et al., 1983) was used to determine the conformation of MgATP that best fit the

experimentally measured internuclear distances. Since no internuclear distances could be measured between the protons on the adenosine and the polyphosphate chain of ATP, we modeled the bound conformation of the adenosine moiety of MgATP using AMP. Distance constraints are utilized to obtain a random trial set of all intramolecular distances. These distances are then used to obtain a set of atomic coordinates that are optimized to give the best agreement possible with the initial distance constraints. The fit of each computed structure to the input data is expressed quantitatively by a score that measures the fourth power of the total deviations of computed and input distances. Usually, 50 solutions are obtained, and acceptable structures are compared to evaluate the uniquess of the conformation determined from the distance constraints. In the conformational search procedure, each atom of AMP was represented by a point at a known distance from the other atoms. If the distance between any two atoms not directly bonded to each other is unknown, its lower bound is set to the sum of the van der Waals radii. The upper bound is set at 40 Å to permit the conformation of the molecule to vary freely. Bond lengths and bond angles, expressed as 1–2 and 1–3 distances, respectively, were obtained from the crystallographic structure of AMP (Neidle et al., 1976). Errors in 1–2 and 1–3 distances were set at 0.01 Å and 0.1 Å, respectively (Rosevear et al., 1983). All dihedral angles were expressed as 1–4 distances and were allowed to vary by 1.5 Å to permit a complete conformational search. Experimental internuclear distances were obtained from Table I. Errors in the distances, Table I, reflect errors both in $f(\tau_r)$ and in the cross-relaxation rates. Because of the sixth root relationship of eq 2, an overall twofold uncertainty in the rates $f(\tau_r)/\sigma_{AB}$ would result in a ±6% error in interproton distances. To ensure planarity of the adenine ring, a subroutine was used that minimizes the weighted sum of the squares of the distances from the best mean plane through the atoms of the adenine ring (Rosevear et al., 1983). The asymmetric ribose carbons were constrained to have the correct chirality by an additional penalty term based on quantitative deviations from the chiral volume. The chiral volume, V_{ch} for each asymmetric carbon atom was calculated according to eq 5, where V_1 and

$$V_{ch} = (V_1 - V_4)\cdot[(V_2 - V_4) \times (V_3 - V_4)] \quad (5)$$

V_4 are the position vectors of the atoms directly bonded to the asymmetric carbon atom, labeled in ascending rank according to the Cahn–Ingold–Prelog system (Havel et al., 1983; Rosevear et al., 1983).

Individual conformations thus computed were evaluated by comparison of internuclear distances with the experimentally determined distance constraints, by comparison of bond lengths and angles with input values, by observing the planarity of the adenine ring, and by the correct chirality of the asymmetric carbon atoms. Of the 50 solutions obtained, 7 had acceptable overall error values to be considered further. The conformation of the ribose ring was evaluated by calculating the five torsional angles of the ribose ring, the phase angle of pseudorotation P, and the backbone torsion angle Ψ (Altona & Sundaralingam, 1972; Levitt & Warshel, 1978). No attempt was made to refine further the calculated structures by any of the available energy minimization routines since enzymes generally do not bind low-energy substrate conformations (Mildvan, 1981) and the nature of the interactions of ATP with creatine kinase is not known in sufficient detail.

Results

Conformation of MgATP Bound to Creatine Kinase. The ribose proton resonances of ATP were unambiguously identified in the presence of 1.3 mM creatine kinase sites by monitoring the proton NMR spectrum and titrating with MgATP to a final concentration of 14.5 mM. The ribose H2′ resonance was obscured by the residual HDO signal and was located by looking for a negative NOE to ribose H1′ in an action spectrum in which the ribose proton region was sequentially irradiated (Figure 1). An NOE is expected between ribose H2′ and H1′ since model building indicates that the distance between them is relatively constant, 2.9 ± 0.2 Å, regardless of either the ribose ring pucker or the glycosidic torsional angle (Rosevear et al., 1983). The ribose region of ATP was sequentially irradiated, and effects on the intensities of the adenine H8 and ribose H1′ protons were monitored (Figure 1). A clear maximum NOE to adenine H8 was observed upon irradiation of either ribose H2′ or ribose H3′, demonstrating that each of these resonances could be selectively irradiated (Figure 1). Similarly, a maximum NOE to ribose H1′ was observed upon irradiation of ribose H4′ (Figure 1). The maximum NOE to either adenine H8 from ribose H3′ or ribose H1′ from ribose H4′ also coincided with the position of these resonances determined from the titration of creatine kinase with ATP. Thus, under the conditions of the NMR experiment the ribose H2′, H3′, and H4′ resonances could be selectively irradiated and the primary NOEs observed from these protons used to calculate internuclear distances. In similar studies performed at low field (250 MHz), where resolution is poorer and potential overlap between resonances greater, selective NOEs from ribose H2′, H3′, and H4′ could also be monitored. Although we cannot unequivocally rule out the possibility that part of the observed NOE could arise from irradiation of underlying protein resonances, a shorter lag period in the buildup of the primary NOE, than is observed in Figure 3, would be expected if the NOE originated from the protons of the protein due to their faster relaxation rates. From the concentrations used, and the dissociation constant of MgATP, K_D = 80 μM (Rosevear et al., 1983), creatine kinase was estimated to be 99% saturated with MgATP under

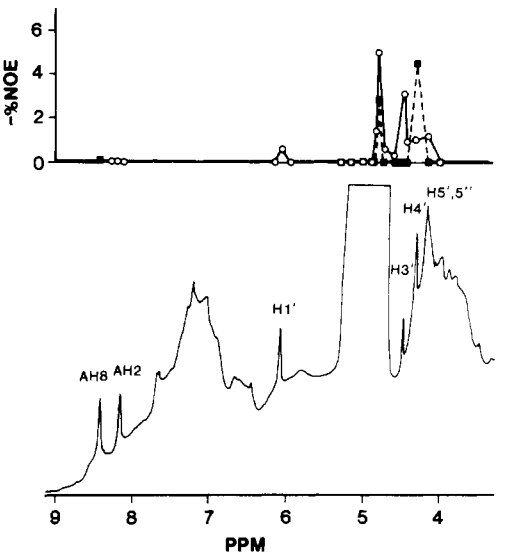

FIGURE 1: Action spectra of interproton nuclear Overhauser effects to adenine H8 and ribose H1′ of MgATP in the presence of creatine kinase. Effects on adenine H8 (○) and ribose H1′ (■) were monitored while the ribose proton region was sequentially preirradiated. A control spectrum is shown on the bottom. The sample contained 1.3 mM rabbit muscle creatine kinase sites and 14.5 mM MgATP in 10 mM Tris-d_{11} buffer containing 0.1 mM DTT at pH 8.0. NOE difference spectra were obtained at 500 MHz from sequentially preirradiating the ribose proton region for 300 ms with 256 scans, 16-bit A/D conversion, 8192 data points, an acquisition time of 0.7 s, a spectral width of 3000 Hz, a relaxation delay of 5 s, and a 90° pulse.

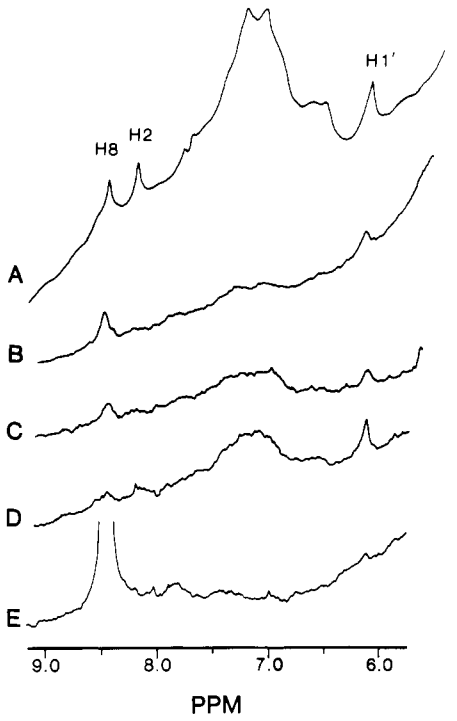

FIGURE 2: Search for interproton NOEs in the aromatic region of the proton NMR spectra of MgATP in the presence of creatine kinase. The sample contained 1.3 mM rabbit muscle creatine kinase sites and 14.5 mM MgATP in 10 mM Tris-d_{11} buffer containing 0.1 mM DTT at pH 8.0. (A) The control spectrum with preirradiation at 10.1 ppm for 150 ms. (B) The NOE difference spectrum obtained from preirradiation of ribose H2′ for 150 ms. All NOE difference spectra are phased with negative NOEs positive and are expanded by a factor of 24. (C) The NOE difference spectrum obtained from preirradiation of ribose H3′ for 150 ms. (D) The NOE difference spectrum obtained from preirradiation of ribose H4′ for 150 ms. (E) The NOE difference spectrum obtained from preirradiation of adenine H8 for 150 ms. NMR spectra were obtained at 500 MHz with 256 scans, 16-bit A/D conversion, 8192 data points, an acquisition time of 0.7 s, a spectral width of 3000 Hz, a relaxation delay of 5 s, and a 90° pulse. A line broadening of 2 Hz was used in processing of all data.

the conditions of the NMR experiment.

Typical 500-MHz protein NMR spectra of 14.5 mM MgATP and 1.3 mM creatine kinase sites are shown in Figure 2. The control spectrum (Figure 2A) was acquired with a preirradation time of 150 ms at 10.1 ppm. The control frequency was chosen to be distant from the MgATP and creatine kinase resonances. Preirradiation of ribose H2′ illustrates the expected negatve interproton NOE to ribose H1′ in the difference spectrum shown in Figure 2B. Irradiation of ribose H2′ also gives a negative NOE to the adenine H8 proton (Figure 2B). Interproton NOEs are also observed in the difference spectrum, from ribose H3′ to adenine H8, upon the preirradiation of ribose H3′ (Figure 2C). Preirradiation of ribose H3′ for 150 ms also results in a small observable NOE to ribose H1′ (Figure 2C). However, this NOE was not observed at the earliest preirradiation time, suggesting that effects from ribose H3′ to H1′ result from secondary effects that cannot easily be used for internuclear distance measurement (Figure 3B) (Noggle & Schirmer, 1971). The longer lag in the secondary NOE to ribose H1′ probably results from the time required to transfer energy from ribose H3′ to H1′ via intermediary spins. Therefore, a time dependence of the NOE development was not calculated, and the cross-relaxation rate from ribose H3′ and H1′ was estimated only as a lower limit. Preirradiation of adenine H8 did not result in any observable NOEs to ribose H1′ (Figure 2E), and conversely, preirradiation of ribose H1′ failed to produce primary NOEs to adenine

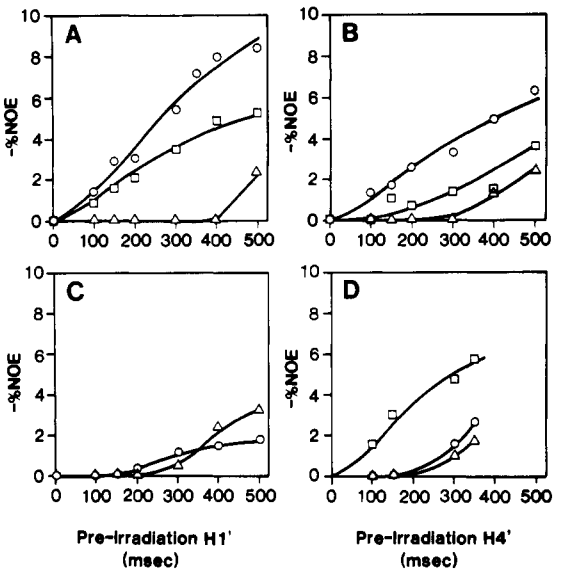

FIGURE 3: Time dependence of the interproton NOEs in MgATP interacting with creatine kinase. (A) Time dependence of NOEs to adenine H8 (○), ribose H1′ (□), and adenine H2 (△) upon preirradiation of ribose H2′. (B) Time dependence of NOEs to adenine H8 (○), ribose H1′ (□), and adenine H2 (△) upon preirradiation of ribose H3′. (C) Time dependence of NOEs to adenine H8 (○) and H2 (△) upon preirradiation of ribose H1′. (D) Time dependence of NOEs to adenine H8 (○), ribose H1′ (□), and adenine H2 (△) upon preirradiation of ribose H4′. Experimental conditions were as described in Figure 2.

Table I: Cross-Relaxation Rates and Interproton Distances on Creatine Kinase Bound MgATP[a]

proton pair (B–A)	ρ_A (s^{-1})	σ_{AB} (s^{-1})	r_{AB} (Å)[b]	r_{AB} (calcd) for structure[c] I	II
H2′–AH8	1.7 ± 0.1	−0.27 ± 0.04	2.8 ± 0.2	2.6	2.6
H3′–AH8	1.7 ± 0.1	−0.18 ± 0.03	3.0 ± 0.2	2.8	3.2
H2′–H1′	4.8 ± 0.4	−0.22 ± 0.03	2.9 ± 0.2[d]	3.0	3.0
H4′–H1′	4.8 ± 0.4	−0.28 ± 0.04	2.8 ± 0.2	2.7	2.8
H3′–H1′	4.8 ± 0.4	≥−0.10	≥3.4	4.0	3.8
H5′–AH8	1.7 ± 0.1	≥−0.08	≥3.5	5.5	4.5
H5″–AH8	1.7 ± 0.1	≥0.08	≥3.5	5.7	4.3
H1′–AH8	1.7 ± 0.1	≥−0.5	≥3.7	3.9	3.9
AH8–H1′	4.8 ± 0.4	≥−0.10	≥3.4	3.9	3.9

[a] Cross-relaxation rates obtained from data of Figure 3. [b] Calculated by using τ_r value of (2.4 ± 0.4) × 10^{-9} s as discussed in the text. [c] Calculated from the two most different best-fit structures of ATP computed by the distance geometry program using the experimentally determined distances. [d] Assumed from X-ray data (2.9 ± 0.2 Å; Rosevear et al., 1983).

H8 (Figure 3C). Observation of primary negative NOEs from ribose H2′ and H3′ to adenine H8 (Figure 3A,B) and the lack of any primary NOEs between ribose H1′ and adenine H8 (Figure 3C) confine the glycosidic torsional angle of bound MgATP to an anti conformation.

The time dependencies of the Overhauser effects were used to separate primary from higher order effects and spin diffusion (Figure 3). The time dependence of the NOEs from ribose H2′ to ribose H1′ and to adenine H8, from ribose H3′ to adenine H8, and from ribose H4′ to ribose H1′ could be fit by the simple two-spin equation (eq 1), by use of the separately measured longitudinal relaxation rates of the protons receiving the NOEs (Table I). Cross-relaxation rates (σ_{AB}) calculated with the data of Figure 3 are given in Table I. Lower limit values of the cross-relaxation rates were estimated

either from the noise level of the data or from the largest observed NOE (Table I).

The transverse relaxation rate ($1/T_2$) of the adenine H8 proton (45 ± 8 s^{-1}), estimated from the line width, was used to set a lower limit on the exchange rate of MgATP from creatine kinase. Since the exchange rate exceeds, by at least an order of magnitude, all of the cross-relaxation rates (Table I), the values of the cross-relaxation rates are not limited by the exchange of MgATP between free and enzyme-bound forms. Therefore, under the conditions of the NMR experiment, the calculated internuclear cross-relaxation rates are those for MgATP bound to creatine kinase.

Internuclear distances were calculated from the individual cross-relaxation rates (Table I) with eq 2 and are given in Table I. The correlation time necessary to calculate interproton distances was obtained from eq 2 and 3 by setting the ribose H2′ to ribose H1′ distance equal to 2.9 ± 0.2 Å, as previously discussed (Rosevear et al., 1983, 1987). This distance has been found, by crystallographic studies, to vary little (±0.2 Å), despite wide variations in ribose ring pucker. By use of the ribose H2′ to H1′ cross-relaxation rate (−0.225 s^{-1}) and a H1′ to H2′ distance of 2.90 Å, a $f(\tau_r)$ of -2.35×10^{-9} was calculated. This $f(\tau_r)$ value yields a correlation time (τ_r) of 2.4×10^{-9} s^{-1}. From eq 3, it can be seen that the correlation function $f(\tau_r)$ is dominated by $-\tau_r$ as expected for high molecular weight systems. Individual correlation times for the ribose H1′ and adenine H8 protons were estimated from the T_1/T_2 ratio by using eq 4 and averaged to yield a τ_r of $(1.5 \pm 0.4) \times 10^{-9}$ s^{-1} for the MgATP–creatine kinase complex. Since greater uncertainty exists in the accurate measurement of T_2, the more precise value of the correlation time, determined from the known ribose H1′ to H2′ distance, was used in eq 2 to calculate all internuclear distances (Table I). However, internuclear distances calculated with the average correlation time obtained from the T_1/T_2 ratio are, within the experimental errors, equal to those reported in Table I. Interproton distances, determined from Overhauser effects, were utilized in model building studies, both by hand and by computer, to determine the conformation of enzyme-bound MgATP.

Model Building of the Conformation of Enzyme-Bound MgATP. A hand-built model of ATP based on the midpoint values of the measured distances (Table I) showed a glycosyl torsional angle $\chi = 75°$ and an O1′-endo ribose pucker. In a more general and objective approach, the experimentally measured internuclear distances were used, together with the previously discussed constraints, in the distance geometry algorithm to determine the conformation of bound MgATP on creatine kinase. This approach also permits the uniqueness of the conformation determined from NMR data to be evaluated. By use of the four internuclear distances and the four lower limit distances (Table I), 75 structures were obtained. Of the 75 structures, only 7 were found to have suitably low deviation from the constrained distances (<12 Å[4]). No attempt was made to further refine the structures. Structures having a larger score were found to contain unusual distortions, such as inappropriate bond lengths, atomic overlap, or a nonplanar adenine ring. The acceptable solutions were further evaluated to determine the glycosidic torsional angle and ribose sugar puckers. All acceptable solutions were found to have a glycosidic torsional angle of 78 ± 10°. However, two classes of solutions were found in comparing the ribose puckers (Table II). The torsional angles, as described by Altona and Sundaralingam (1972) and Levitt and Warshel (1978), were calculated, and the pseudorotation phase angles

Table II: Calculated Values of Ribose Torsional Angles and Phase Angle of Pseudorotation P for the Two Best-Fit Most Different Computed Structures of Bound MgATP[a]

torsional angle	symbol	angle (deg) structure I	structure II
C4′–O4′–C1′–C2′	τ_0	−23.9	−25.4
O4′–C1′–C2′–C3′	τ_1	9.9	−0.8
C1′–C2′–C3′–C4′	τ_2	7.4	25.0
C2′–C3′–C4′–O4′	τ_3	−21.5	−42.3
C3′–C4′–O4′–C1′	τ_4	26.7	41.8
O4′–C1′–N9–C8	χ	81	75
O5′–C5′–C4′–C3′	γ	−140 (*gt*)	70 (*gg*)
pseudorotation phase	P	74	54
backbone torsion angle	Ψ[b]	98	78

[a] The glycosidic torsion angles χ and the conformation of the C5′–O5′ side chain (γ) are also shown. [b] Definition of angles taken from Levitt and Warshel (1978) and Altona and Sundaralingam (1972).

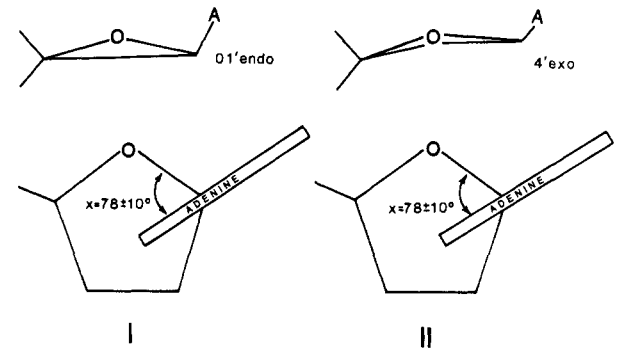

FIGURE 4: Comparison of the two alternative conformations for the ribose ring pucker and the glycosidic torsional angle of enzyme-bound MgATP computed by the distance geometry algorithm, using the experimentally measured internuclear distances (Table I).

of ribose were determined for all the acceptable structures. The pseudorotation phase angles were found to be centered around 55° and 75°. The torsional angles and the pseudorotation phase angle of the best solution from each class of structures are given in Table II. Phase angles of 54° and 74° correspond to ribose C4′-exo and ribose O1′-endo sugar puckers, respectively (Figure 4). Backbone torsional angles (Ψ = 78° and 98°) also correspond to ribose C4′-exo and ribose O1′-endo sugar puckers, respectively (Levitt & Warshel, 1978). Orientations about the C4′–C5′ bond (γ) were found to be either gauche,gauche or gauche,trans (Table II, Figure 4). Although the NOE data can be fit with either a C4′-exo or O1′-endo ribose pucker, we cannot unambiguously rule out a mixture of ribose conformations which yield distances that are consistent with both conformations. Both classes of structures (Table II) are consistent with distances determined by the paramagnetic probe–T_1 method, from the unpaired electron of a nitroxide spin-label to the adenine H8 and H2 and ribose H1′ protons of MgADP (McLaughlin et al., 1976). This consistency suggests a unique conformation about the glycosidic bond.

Discussion

The combination of internuclear distances obtained from nuclear Overhauser effects and computer model building was used to define the conformation of MgATP bound to rabbit muscle creatine kinase. The internuclear distances (Table I) were sufficiently precise to define uniquely the glycosidic torsional anggle (χ = 78 ± 10°) but insufficient to define uniquely the ribose ring pucker. Both C4′-exo and O1′-endo ribose puckers were found to be consistent with the experimentally measured distances. However, an interconverting

mixture of ribose sugar puckers could not be ruled out for MgATP bound to creatine kinase. This is a reasonable possibility with creatine kinase, since the Mn^{2+} complexes of ADP, 2′dATP, and 3′ADP differ by a factor of at most 3 in substrate activity and in binding to this enzyme (O'Sullivan & Cohn, 1966). On other enzymes, specific interactions between the ribose ring and the protein might be expected to confine the ribose ring to a unique structure. Model building studies on the tyrosyl-tRNA synthetase–tyrosyl adenylate complex, using crystallographic data, have revealed several potential hydrogen bonds between the ribose of the substrate and the synthetase (Leatherbarrow et al., 1985). Some of these potential hydrogen bonds have been confirmed by mutagenesis studies (Wilkinson et al., 1983; Leatherbarrow et al., 1985; Fersht et al., 1986). It is also well-known that minor alterations in the ribose ring can greatly affect the ability of several other enzymes to utilize the modified nucleotides. Such studies suggest that many nucleotides binding proteins may interact with the ribose in a specific manner that uniquely restricts its ring pucker. NMR studies have previously suggested an O1′-endo pucker for ATP bound to protein kinase (Rosevear et al., 1983) and for dATP and TTP bound to DNA polymerase I (Ferrin & Mildvan, 1985).

The unique high anti-glycosidic torsional angle ($\chi = 78 \pm 10°$) found for MgATP bound to creatine kinase is consistent with the known preference of creatine kinase for ATP compared to other nucleoside triphosphates. Enzymes exhibiting high nucleotide specifity for ATP, protein kinase ($\chi = 78 \pm 10°$) (Rosevear et al., 1983), and adenylate kinase ($\chi =$ 60–65°) (Fry et al., 1985) have also been found to bind ATP with an unique high anti-glycosidic torsional angle. However, multiple conformations about the glycosidic torsional angle of MgATP bound to pyruvate kinase have been found (Rosevear et al., 1987), consistent with the relatively nonspecific utilization of purine and pyrimidine nucleotide substrates by this enzyme (Plowman & Krall, 1965). Thus, creatine kinase is another enzyme that fits the general correlation, first noted by Mildvan (1981), that enzymes which exhibit a high nucleotide specificity hold the nucleotide in a unique conformation about the glycosidic bond.

The use of the distance geometry algorithm to determine the conformation of enzyme-bound nucleotides permits all possible conformations, consistent with the experimentally determined constraints, to be searched. Acceptable solutions can be compared quantitatively and the allowed conformational space of the bound nucleotide objectively defined. Computer studies replacing the measured distances of Table I with upper limit distances (≤3.4 Å in the presence case) and lower limit distances (2.2 Å based on the van der Waals sum) suggest that the allowed range of glycosidic torsional angles for the bound nucleotide can be defined with almost the same degree of accuracy as obtained with the measured distances. This approach has yielded the correct range of allowed adenine–ribose conformations for ATP bound to creatine kinase as well as to protein kinase. However, as expected, the range of allowed ribose sugar puckers is found to be greater. This simpler method will probably be more applicable when the upper limit distances are relatively low, as in the present case.

The present data, which show a unique high anti-glycosidic torsional angle ($\chi = 78 \pm 10°$) for bound MgATP on creatine kinase, along with previous paramagnetic probe–T_1 data (McLaughlin et al., 1976), the location of the divalent cation activator (Reed & Leyh, 1980; Leyh et al., 1985), and the nature and location of the general acid/base catalyst (Rosevear et al., 1981) will be of value in elucidating the overall arrangement of substrates at the active site of creatine kinase and will facilitate the positioning of MgATP into the X-ray structure of the enzyme, when it becomes available.

References

Altona, C., & Sundaralingam, M. (1972) *J. Am. Chem. Soc. 94*, 8205.

Borders, C. L., Jr., & Riordan, J. F. (1975) *Biochemistry 14*, 4699.

Clarke, D. E., & Price, N. C. (1979) *Biochem. J. 181*, 467.

Clore, G. M., & Gronenborn, A. M. (1983) *J. Magn. Reson. 53*, 423.

Cook, P. F., Kenyon, G. L., & Cleland, W. W. (1981) *Biochemistry 20*, 1204.

DeLeeuw, H. P. M., Haasnoot, C. A. G., & Altona, C. (1980) *Isr. J. Chem. 20*, 108.

Ferrin, L., & Mildvan, A. S. (1985) *Biochemistry 24*, 6904.

Ferrin, L., & Mildvan, A. S. (1986) *Biochemistry 25*, 5131.

Fersht, A. R., Leatherbarrow, R. J., & Wells, T. N. C. (1986) *Nature (London) 322*, 284.

Fry, D. C., Kuby, S. A., & Mildvan, A. S. (1985) *Biochemistry 24*, 4680.

Hammes, G. G., & Hurst, J. K. (1969) *Biochemistry 8*, 1083.

Havel, T. F., Kuntz, I. D., & Crippen, G. M. (1983) *Bull. Math. Biol. 45*, 665.

Hershenson, S., Helmers, N., Desmeules, P., & Stroud, P. (1986) *J. Biol. Chem. 261*, 3732.

James, T. L. (1976) *Biochemistry 15*, 4724.

James, T. L., & Cohn, M. (1974) *J. Biol. Chem. 249*, 2599.

Kalk, A., & Berendsen, H. J. L. (1976) *J. Magn. Reson. 24*, 343.

Kenyon, G. L., & Reed, G. H. (1983) *Adv. Enzymol. Relat. Areas Mol. Biol. 54*, 367.

Kuntz, I. D., Crippen, G. M., & Kollman, P. A. (1979) *Biopolymers 18*, 939.

Leatherbarrow, R. J., Fersht, A. R., & Winter, G. (1985) *Proc. Natl. Acad. Sci. U.S.A. 82*, 7840.

Levitt, M., & Warshel, A. (1978) *J. Am. Chem. Soc. 100*, 2607.

Levy, H. R., Ejchart, A., & Levy, G. C. (1983) *Biochemistry 22*, 2792.

Leyh, T. S., Goodhart, P. J., Nguyen, A. C., Kenyon, G. L., & Reed, G. H. (1985) *Biochemistry 24*, 308.

McLaughlin, A. C., Leigh, J. S., & Cohn, M. (1976) *J. Biol. Chem. 251*, 2777.

Mildvan, A. S. (1981) *Philos. Trans. R. Soc. London, B 293*, 65.

Mildvan, A. S., Granot, J., Smith, G. M., & Liebman, M. N. (1980) *Adv. Inorg. Biochem. 2*, 211.

Mildvan, A. S., Rosevear, P. R., Granot, J., O'Brian, C. A., Bramson, H. N., & Kaiser, E. T. (1983) *Methods Enzymol. 99*, 93.

Morrison, J. F., & James, E. (1965) *Biochem. J. 97*, 37.

Morrison, J. F., & Cleland, W. W. (1966) *J. Biol. Chem. 241*, 673.

Noda, L., Kuby, S. A., & Lardy, H. A. (1954) *J. Biol. Chem. 209*, 203.

Noggle, J. H., & Schirmer, R. E. (1971) *The Nuclear Overhauser Effect*, Academic, New York.

O'Sullivan, W. J., & Cohn, M. (1966) *J. Biol. Chem. 241*, 3116.

Plowman, K. M., & Krall, A. R. (1965) *Biochemistry 4*, 2809.

Pradel, L. A., & Kassab, R. (1968) *Biochim. Biophys. Acta 167*, 317.

Reed, G. H., & Leyh, T. S. (1980) *Biochemistry 19*, 5472.

Rosevear, P. R., Bramson, H. N., O'Brian, C., Kaiser, E. T.,

& Mildvan, A. S. (1983) *Biochemistry 22*, 3439.
Rosevear, P. R., Sellin, S., Mannervik, B., Kuntz, I. D., & Mildvan, A. S. (1984) *J. Biol. Chem. 259*, 11436.
Rosevear, P. R., Fox, T. L. & Mildvan, A. S. (1987) *Biochemistry 26*, 3487–3493.
Schimerlik, M. I., & Cleland, W. W. (1973) *J. Biol. Chem. 248*, 8418.
Tanzer, M. L., & Gilvarg, C. (1959) *J. Biol. Chem. 234*, 3201.
Tropp, J., & Redfield, A. G. (1981) *Biochemistry 20*, 2133.
Vasak, M., Nagoyama, K., Wüthrich, K., Mertens, M. L., & Kagi, J. H. R. (1979) *Biochemistry 18*, 5050.
Wagner, G., & Wüthrich, K. (1979) *J. Magn. Reson. 33*, 675.
Wilkinson, A. J., Fersht, A. R., Blow, D. M., & Winter, G. (1983) *Biochemistry 22*, 3581.

Synthesis of a Phosphorothioate Analogue of Flavin Mononucleotide: Reconstitution of the FMN-Free Form of NADPH–Cytochrome P-450 Reductase†

Judith Porter Calhoun,‡ Henry M. Miziorko,‡ James D. Otvos,§ David P. Krum,‡ Steven Ugent,‡ and Bettie Sue Siler Masters*,‡

Department of Biochemistry, Medical College of Wisconsin, Milwaukee, Wisconsin 53226, and Department of Chemistry, University of Wisconsin—Milwaukee, Milwaukee, Wisconsin 53201

Received December 17, 1986; Revised Manuscript Received April 8, 1987

ABSTRACT: The chemical synthesis of riboflavin 5′-phosphorothioate (5′-FMNS) is described. 5′-FMNS is obtained from the alkaline hydrolysis of riboflavin 4′,5′-cyclic phosphorothioate, which is produced upon reaction of riboflavin (RB) with thiophosphoryl chloride in trimethyl phosphate. 5′-FMNS has been tested for enzymatic reconstitution of NADPH–cytochrome P-450 reductase (EC 1.6.2.4) depleted of its FMN prosthetic group, but containing its full complement (1 equiv) of FAD. The synthesis, purification, and characterization of 5′-FMNS are reported, and documentation of its efficacy in reconstituting the reductase by fluorometric and absorbance spectrophotometric measurements, as well as enzymatic activity, is presented. Data indicate that 5′-FMNS is totally competent in reconstituting NADPH–cytochrome *c* reductase activity, which requires the presence of both FAD and a flavin mononucleotide, and its fluorescence is completely quenched upon addition to FMN-free NADPH–cytochrome P-450 reductase.

The use of structurally modified substrates and coenzyme analogues in the investigation of enzyme mechanisms, structure, and function has increased in recent years. Much attention has been focused on the use of modified nucleotides in mechanistic studies. One particular class of nucleotide analogues that is very useful in mechanistic studies is that of nucleoside phosphorothioates, first introduced by Eckstein (1979, 1985). These are compounds in which a nonbridging oxygen atom of a phosphate group has been replaced by a sulfur atom. Large numbers of phosphorothioate derivatives have been synthesized and applied to the study of various enzyme systems (Eckstein, 1985).

In the study of flavoproteins, modified flavin analogues have been very useful in unraveling the role of the isoalloxazine ring of the flavin in the binding of the flavin to the flavoprotein and in its participation in the catalytic mechanism of the flavoprotein in question (Ghisla & Massey, 1986). A few examples are the use of 6-substituted flavins (Ghisla et al., 1986), 1-carba-1-deazariboflavin (1-deazariboflavin; Spencer et al., 1977), 5-deazaflavins (Edmondson et al., 1972; Fisher et al., 1976), and ^{13}C and ^{15}N isotopically substituted flavins (Vervoort et al., 1985; Moonen et al., 1984a,b; Franken et al., 1984; Van Schagen & Müller, 1981). In their review of "artificial" flavins as active-site probes, Ghisla and Massey classified the various analogues into four categories on the basis of the type of information obtained: spectral probes, chemically active probes, mechanistic probes, and photoaffinity labels.

Since the work in McCormick's laboratory in the 1960s (McCormick et al., 1964; Tsibris et al., 1965, 1966; Roth et al., 1966), very little emphasis has been placed on substitutions aside from those directly involving the isoalloxazine ring with the exception of the 8-azido- (adenine) FAD, which has been used as a photoaffinity label for D-amino acid oxidase (Koberstein, 1976). During our investigation of NADPH–cytochrome P-450 reductase, the only mammalian flavoprotein known to contain 1 mol each of FAD and FMN, we became interested in studying the effects of a phosphorothioate moiety in the ribityl side chain of FMN on the catalytic, spectral, and fluorescent properties of the enzyme. In this paper, the chemical synthesis and characterization of riboflavin 5′-monophosphorothioate (5′-FMNS) and preliminary studies of its interaction with FMN-depleted NADPH–cytochrome P-450 reductase are reported. This is the first report of a flavin phosphorothioate analogue utilized in reconstituting a flavoprotein.

Materials and Methods

General. FAD, FMN, Trizma base, and cytochrome *c* (type VI) were purchased from Sigma Chemical Co. The flavins were purified by DEAE chromatography and shown to be >95% pure by the reverse-phase HPLC procedure of Light et al. (1980) as detected by absorbance at 444 nm. FAD was shown to be homogeneous, and FMN preparations were shown to contain 86% 5′-FMN and 14% 4′-FMN by ^{31}P NMR. NADPH was obtained from Pharmacia P-L Biochemicals.

† Supported by a grant from the National Institutes of Health (HL 30050) to B.S.S.M.
‡ Medical College of Wisconsin.
§ University of Wisconsin—Milwaukee.

0006-2960/87/0426-5344$01.50/0